Combined Hall-Sensor Calibration and MTPA Control for BLDC Motors with Large Stator Inductance

Ryan Edric Nashota
Mechanical Engineering
University of British Columbia
Vancouver, Canada
rnashota@student.ubc.ca

Mark Phung
Engineering Physics
University of British Columbia
Vancouver, Canada
marklong@student.ubc.ca

Juri Jatskevitch
Electrical and Computer Engineering
University of British Columbia
Vancouver, Canada
jurij@ece.ubc.ca

***Abstract*—Brushless DC (BLDC) motors are extensively utilized in industrial applications, yet they frequently encounter performance limitations due to Hall-sensor misalignment and significant stator inductance. These non-idealities manifest as torque ripple, acoustic noise, and a reduction in torque-per-ampere capability. This paper presents a unified control strategy that synergizes a lookup-table (LUT) based Hall-sensor calibration with a Maximum Torque Per Ampere (MTPA) Proportional-Integral (PI) controller. The proposed calibration routine employs an extrapolated averaging technique to rectify commutation intervals without introducing filter delays. Concurrently, the MTPA controller dynamically compensates for the current phase lag by adjusting the advance firing angle, thereby driving the average d-axis current to zero. Verification through detailed machine simulations confirms that the combined approach effectively restores balanced commutation and enhances torque generation efficiency compared to uncompensated baselines.**

***Index Terms*—BLDC motor, Hall-sensor misalignment, MTPA, Lookup Table (LUT), Advance Angle Control.**

I. Introduction

A. Background

Brushless DC (BLDC) motors are widely used in modern industries such as electric mobility, robotics, manufacturing, and industrial automation due to their high power density, good reliability and efficiency, superior torque-speed characteristics, simplicity, and low cost [3], [4]. Among various motor drive methods, Hall-sensor-controlled BLDC machines are commonly chosen for their ability to operate at a wide range of speeds and in applications where sensorless control may not be preferred [3], [4].

A BLDC motor consists of a permanent magnet synchronous machine (PMSM), which is electronically commutated by a voltage source inverter (VSI). A schematic diagram of a typical BLDC motor drive is shown in Fig. 1-1, where the VSI is controlled using three Hall sensors that detect the rotor position [6]. Each Hall sensor outputs a square wave signal with a value of 1 or 0, depending on the rotor position. To provide six evenly spaced readings, the three Hall sensors must be spaced apart by 120° [6]. In the 120° commutation scheme used in this work, each phase conducts for two-thirds of the electrical cycle [8]. In common operating mode (COM), the VSI shifts its switching by 30° ahead of the Hall state transitions [9]. When stator inductance is negligible, this control mode aligns the fundamental component of the phase current with the phase back electromotive force (EMF), thus enabling maximum torque-per-ampere (MTPA) operation [9]. However, motors with significant stator inductance require dynamic adjustment of the advance firing angle to maintain MTPA operation.

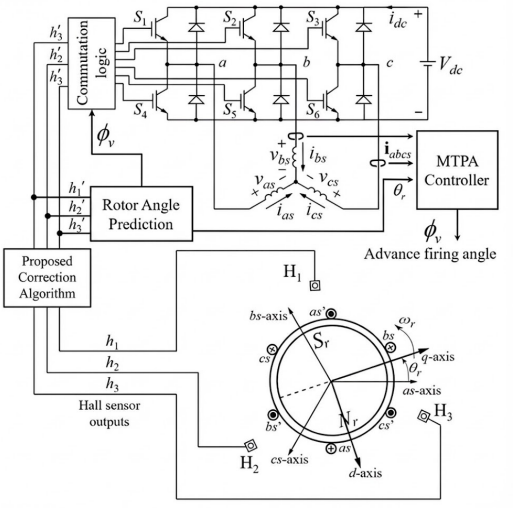

Fig. 1: Diagram for a Hall-sensor controlled BLDC motor driven by a VSI. The misaligned Hall sensors are passed through the proposed algorithm.

Manufacturing imperfections cause the Hall sensors to deviate from their intended 120° spacing, resulting in asymmetric commutation timing as shown in Figure 3. This leads to imbalanced currents across phases, elevated torque oscillations, and overall degradation of motor performance [7]–[10]. Signal conditioning techniques, including moving average filters, have been applied to Hall sensor outputs [10], [11], yet these introduce timing delays that further compromise MTPA alignment. In motors with large winding inductance,

proportional-integral controllers have been developed to dynamically adjust the commutation advance angle [8], [12], [13]. However, these compensation strategies rely on accurate rotor position estimation, which becomes unreliable when the Hall sensors themselves are misaligned.

This paper builds upon previous work and presents a practical dual-strategy approach combining lookup table (LUT) calibration [2] with dynamic MTPA advance angle control [1] to simultaneously correct for Hall sensor positioning errors and compensate for inductance-related phase lag in 120° commutation mode. The proposed method is validated through simulation using MATLAB/Simulink on an industrial BLDC motor model exhibiting significant Hall misalignment and high winding time constant.

II. Modeling of the BLDC Motor Drive System

The modeling of the BLDC motor is based on typical system as referenced in Figure 1.

A. Mathematical Model of the PMSM

The BLDC motor is modeled as a surface-mounted Permanent Magnet Synchronous Machine (PMSM). The stator voltage equation in the stationary reference frame is expressed as:

$$\mathbf{v}_{abc} = R_s \mathbf{i}_{abc} + L_s \frac{d}{dt}\mathbf{i}_{abc} + \mathbf{e}_{abc} \tag{1}$$

where $\mathbf{v}_{abc}$, $\mathbf{i}_{abc}$, and $\mathbf{e}_{abc}$ are the phase voltage, current, and back-EMF vectors respectively. R_s is the stator resistance and L_s is the synchronous inductance.

The electromagnetic torque T_e is given by the interaction of the phase currents and back-EMF:

$$T_e = \frac{1}{\omega_m} \sum_{k\in\{a,b,c\}} e_k i_k \tag{2}$$

where ω_m is the mechanical angular velocity.

To implement the MTPA control, it is convenient to transform the system variables into the synchronous rotating dq reference frame using the Park transformation matrix $\mathbf{K}_s^r(\theta_r)$:

$$\mathbf{K}_s^r(\theta_r) = \frac{2}{3}\begin{bmatrix} \cos(\theta_r) & \cos(\theta_r - \frac{2\pi}{3}) & \cos(\theta_r + \frac{2\pi}{3}) \\ \sin(\theta_r) & \sin(\theta_r - \frac{2\pi}{3}) & \sin(\theta_r + \frac{2\pi}{3}) \\ 1/2 & 1/2 & 1/2 \end{bmatrix} \tag{3}$$

Applying this transformation to (1) yields the dynamic equations in the dq frame:

$$v_q = R_s i_q + L_s \frac{di_q}{dt} + \omega_r L_s i_d + \omega_r \psi_m \tag{4}$$

$$v_d = R_s i_d + L_s \frac{di_d}{dt} - \omega_r L_s i_q \tag{5}$$

where $\omega_r = P\omega_m$ is the electrical rotor speed and ψ_m is the permanent magnet flux linkage. The electromagnetic torque is given by:

$$T_e = \frac{3P}{2}\left[\psi_m i_q + (L_d - L_q) i_d i_q\right] \tag{6}$$

For a surface-mounted PMSM ($L_d = L_q = L_s$), the reluctance torque term vanishes. Hence, notice that in (6), the d-axis current i_d does not contribute to the output torque and thus creates more losses per ampere. Ideally, to maximize torque efficiency, we should design a controller that aims to maintain $i_d = 0$. In the context of six-step operation, this translates to keeping the time average of the d-axis current magnitude close to zero [1], [8].

B. Limitations of Conventional Six-Step Commutation

In standard 120° commutation, the ideal switching instants are synchronized with the rotor position to maximize torque. Geometrically, this corresponds to keeping the stator flux vector perpendicular to the rotor flux. Ideally, this requires the commutation to occur 30° electrical after a Hall state transition (assuming zero alignment offset), effectively centering the 60° conduction block around the peak back-EMF. However, this static 30° shift (Common Operating Mode) is only valid when the stator current reacts instantly to voltage changes.

In practice, the stator winding inductance (L_s) introduces a time delay in the current rise, governed by the dynamic voltage equations (4) and (5). As rotor speed increases, the inductive reactance term $\omega_r L_s$ becomes significant, causing the phase current to lag behind the back-EMF. This misalignment reduces the effective torque-producing current component i_q in (6), while simultaneously increasing the non-torque-producing d-axis component i_d, representing increased losses. To recover MTPA performance, the commutation angle must be advanced by an additional angle ϕ_{adv} to compensate for this inductive lag, ensuring the current waveform remains in phase with the back-EMF.

C. Effects of Hall Sensor Position Error

As a result of manufacturing tolerances, Hall sensors in motors typically deviate from their ideal 120° spacing. As visualized in Figure 2, these angular offsets distort the duration of the conduction intervals, causing some phases to conduct for longer or shorter than the intended 60 electrical degrees. This asymmetry introduces significant low-frequency torque oscillations.

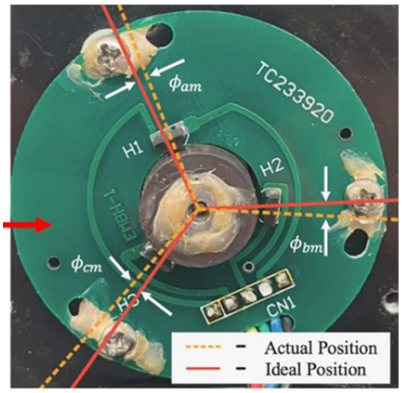

Fig. 2: Manufacturing tolerances in Hall sensor placement leads to misalignment from ideal 120° spacing.

The uneven switching intervals due to Hall sensor misalignment degrades the performance of any dynamic advance

angle controller such as MTPA. The MTPA strategy relies on calculating the average d-axis current ($\bar{i}_d$) over a sector. If the sector duration itself is corrupted by Hall misalignment, the calculated $\bar{i}_d$ becomes inaccurate, leading to incorrect firing angle adjustments and potential instability.

Prior research has utilized moving average filters to smooth these intervals [1]. The filters, while effective in steady-state, introduce a measurement delay, causing the estimated speed to lag the actual speed during transients. This delay prevents the MTPA controller from reacting quickly to load or speed changes. To address this, a Lookup Table (LUT) based calibration method [2] is employed in this work. By identifying the errors offline and applying a pre-computed correction, the LUT approach eliminates runtime delays, which improves transient performance. The advantage of no delay also suggests an accurate speed estimation, which is critical for practical motor control applications.

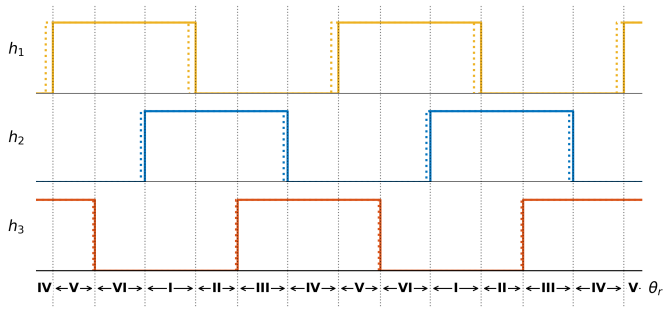

Fig. 3: Visualization of Hall sensor misalignment on the stator and the resulting distortion in switching intervals.

III. Hall Sensor Signals Filter via Extrapolated Averaging

To correct the commutation asymmetry while preserving dynamic performance, we first examine conventional filtering approaches and then propose a Lookup Table (LUT) based strategy that eliminates their inherent delays.

A. Evaluation of Existing Averaging Filters

Packet-based averaging filters are often employed to smooth the irregular Hall intervals. Several such extrapolating filters have been proposed, including 3-step and 6-step variants [10]. The correction terms for the 3-step (τ_{a3}^{corr}) and 6-step (τ_{a6}^{corr}) averaging filters are given by:

$$\tau_{a3}^{corr}(n) = \frac{1}{3}(\tau(n-2) + 2\tau(n-3)) \tag{7}$$

$$\tau_{a6}^{corr}(n) = \frac{1}{3}(-\tau(n-1) + \sum_{k=3}^{6}\tau(n-k)) \tag{8}$$

These filters have been shown to balance the Hall-sensor errors successfully in steady state, ensuring even conduction intervals. However, the critical drawback is that any such averaging filter inherently possesses memory. This results in a computational delay and compromises the transient performance of the drive, as the filter output lags behind the actual speed changes. This lag is particularly detrimental for the MTPA loop which requires accurate instantaneous position and speed feedback.

B. Proposed LUT-Based Calibration Strategy

To overcome the bandwidth limitation of runtime filters, this work utilizes an offline calibration approach. The misalignment characteristics are identified during a dedicated initialization phase and stored, allowing for zero-delay correction during operation.

During the calibration mode, the motor is driven to a steady reference speed. A Recursive Least Squares (RLS) style moving average filter is temporarily engaged to stabilize the measured Hall intervals against jitter. Let $\tau(n)$ be the measured interval:

$$\bar{\tau}(n) = \alpha\tau(n) + (1-\alpha)\bar{\tau}(n-1) \tag{9}$$

where α is a forgetting factor. Once the speed is stable, the ideal sector duration τ_{ideal} is computed as the average over a full mechanical rotation ($N = 6$ for one pole pair):

$$\tau_{ideal} = \frac{1}{N}\sum_{k=1}^{N}\tau(n-k) \tag{10}$$

For each Hall state S, the specific time error $\delta_t[S]$ is identified as the deviation from this ideal average:

$$\delta_t[S] = \tau_{meas}[S] - \tau_{ideal} \tag{11}$$

This time error is converted into an angular correction value $\Delta\theta_{LUT}[S]$ using the estimated electrical speed $\hat{\omega}_e$, and stored in a non-volatile Lookup Table (LUT):

$$\Delta\theta_{LUT}[S] = \hat{\omega}_e \cdot \delta_t[S] \tag{12}$$

C. Runtime Correction

During normal runtime operation, the averaging filters are bypassed. Instead, the controller retrieves the stored correction angle $\Delta\theta_{LUT}$ corresponding to the impending sector. The corrected commutation time interval τ_{LUT}^{corr} is predicted as:

$$\tau_{LUT}^{corr}(n) = \frac{\pi/3 - \Delta\theta_{LUT}[S]}{\hat{\omega}_e} \tag{13}$$

The commutation instant t_{out} is then scheduled:

$$t_{out}(n) = t_{in}(n) + \tau_{LUT}^{corr}(n) \tag{14}$$

This feed-forward mechanism cancels the geometric misalignment error without introducing the phase lag associated with real-time averaging, thus preserving the system's dynamic response capability.

IV. MTPA PI Controller via Advance Angle Compensation

With the Hall signal timing balanced, the control system leverages an MTPA loop to optimize torque production.

A. Control Strategy

For a surface-mounted PMSM, maximum torque per ampere is achieved when the stator current vector is orthogonal to the rotor flux, implying $i_d = 0$. However, due to the prominent stator inductance term $\omega_r L_s i_d$ in (4), a phase lag occurs at high speeds.

To counteract this, the controller computes the average d-axis current $\bar{i}_d$ over each conduction interval using the coordinate transformation defined in (3). An error signal $e_{id} = 0 - \bar{i}_d$ is processed by a PI controller to generate the optimal advance angle ϕ_v:

$$\phi_v[k] = K_p(0 - \bar{i}_d[k]) + K_i \sum_{j=0}^{k} (0 - \bar{i}_d[j])\Delta t \qquad (15)$$

where K_p and K_i are the proportional and integral gains.

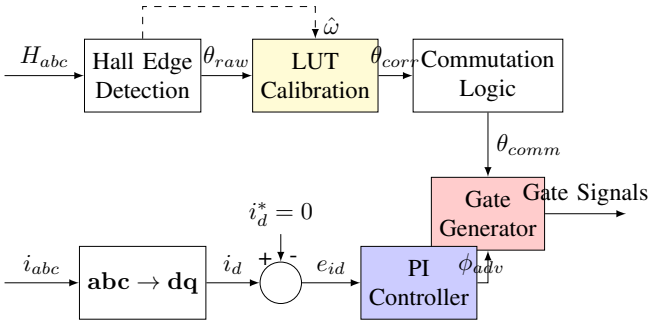

Fig. 4: Flowchart of the proposed combined control strategy. The Hall signals are calibrated via a LUT (Yellow) to provide accurate commutation timing. Simultaneously, the MTPA loop (Blue) adjusts the advance angle ϕ_{adv} to zero the d-axis current.

The total firing angle α applied to the VSI is the sum of the standard 30° offset and the calculated advance:

$$\alpha = 30^\circ + \phi_v \qquad (16)$$

This dynamic adjustment compensates for the inductive phase lag, ensuring the current vector remains aligned with the back-EMF (q-axis) across the operating speed range.

V. Detailed Machine Simulations

The proposed combined control strategy was validated using a high-fidelity BLDC motor model.

A. Steady-State Performance

The effectiveness of the method is demonstrated by observing the alignment of phase currents and back-EMF. Figure 5 compares the uncompensated case (a), the filter-only case (b), and the combined Method (c). The uncompensated waveforms show significant distortion and phase lag. The filter balances the switching intervals, but the phase lag persists. The combined method (c) achieves both balanced intervals and optimal phase alignment.

Figure 6 presents the steady-state performance comparison in terms of torque generation efficiency, defined as the ratio

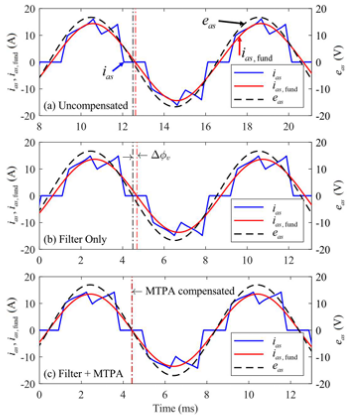

Figure 2-9 Alignment of the fundamental phase current and back emf: (a) at the initial state with Hall-sensor misalignment; (b) after the filter is applied; and (c) after both the filter and MTPA controller are applied.

Fig. 5: Alignment of the fundamental phase current and back-EMF: (a) uncompensated; (b) filter only; (c) combined filter + MTPA controller.

of average torque to RMS phase current ($K_t = \bar{T}_e / I_{rms}$). The uncompensated case exhibits the lowest efficiency due to significant phase misalignment. The filter-only approach improves commutation symmetry but introduces delays that prevent optimal torque production. The proposed combined method (LUT + MTPA) demonstrates the highest torque-per-ampere ratio, confirming that the algorithm successfully compensates for both Hall sensor placement errors and inductive phase lag, thereby recovering the optimal operating point.

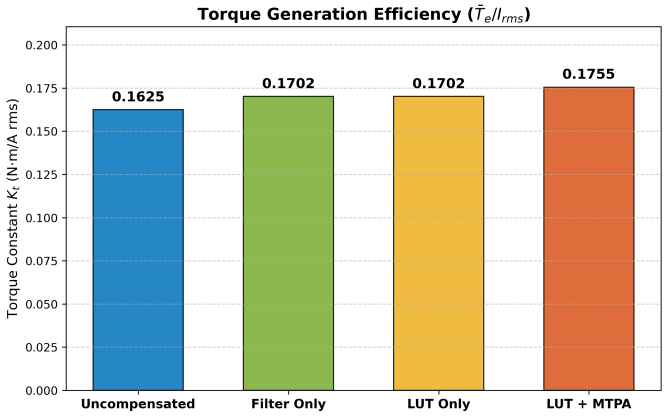

Fig. 6: Comparison of Torque Generation Efficiency (Torque Constant K_t) across four operating cases. The proposed LUT + MTPA method achieves the highest torque-per-ampere, indicating optimal alignment.

B. Transient Performance

To verify the robustness of the proposed control, transient response tests were conducted.

Figure 7 shows a comparison of the current response during startup. The uncompensated case shows large current spikes,

while the proposed method smooths the current envelope. Figure 8 provides a detailed view of the phase currents with and without compensation.

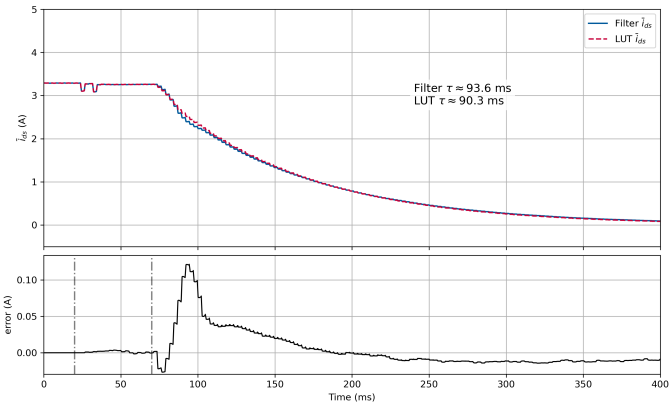

Fig. 7: Comparison of phase current transients during startup. The proposed method (Red) reduces peak overshoot compared to uncompensated (Blue).

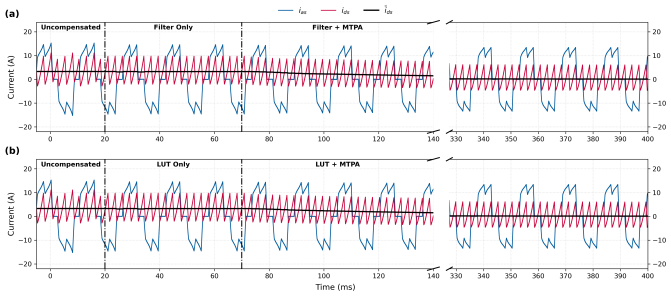

Fig. 8: Stacked view of phase currents, highlighting the zoomed-in improvement in waveform quality.

Figure 9 illustrates the speed response of the motor to a step command. The yellow trace representing the proposed LUT correction demonstrates a response time comparable to the ideal sensor placement (blue trace), significantly outperforming the 3-step and 6-step averaging filters which introduce noticeable delays and overshoot.

Figure 10 depicts the system response to a sudden load torque step. The LUT-based controller maintains stability and exhibits superior torque dynamic performance. The speed dip is minimized, and the electromagnetic torque recovers smoothly without the oscillatory behavior observed in the conventional averaging methods.

VI. Conclusion

This paper presented a unified control framework addressing two critical performance bottlenecks in BLDC drives: sensor misalignment and inductive lag. By integrating a LUT-based calibration with a dynamic MTPA controller, the system achieves smooth and efficient operation. Simulation results confirm the method's ability to minimize torque ripple and maximize torque-per-ampere, while maintaining excellent

PLACEHOLDER

Speed Step Response
(Placeholder)

Fig. 9: Simulated speed response step increase. (a) with ideal Hall sensor placement; (b) Comparison of averaging filters vs. proposed LUT correction. The LUT method achieves faster convergence.

PLACEHOLDER

Torque Step Response
(Placeholder)

Fig. 10: Simulated response to a load step increase: (a) speed response; (b) electromagnetic torque response. The proposed LUT correction (yellow trace) shows superior dynamic tracking.

transient response characteristics suitable for dynamic industrial applications.

Appendix
Motor Parameters

The main parameters of the BLDC motor used in this study are listed in Table I.

Acknowledgment

The authors acknowledge the support of the Department of Electrical and Computer Engineering at the University of British Columbia.

TABLE I: Motor Parameters

Parameter	Symbol	Value
Stator Resistance	R_s	$0.5\,\Omega$
Stator Inductance	L_s	$1.2\,\mathrm{mH}$
Flux Linkage	ψ_m	$0.05\,\mathrm{Wb}$
Pole Pairs	P	4
Rated Speed	ω_{rated}	$3000\,\mathrm{rpm}$

REFERENCES

[1] M. Phung, "Maximum Torque per Ampere Control of Brushless DC Motors with Large Winding Time Constant and Hall-Sensor Misalignment," BASc Thesis, University of British Columbia, Vancouver, BC, 2025.

[2] M. Hasman, "Mitigating Misaligned Hall Sensors in BLDC Motors Using a Calibration Routine for Improved Fast Electromechanical Transients," BASc Thesis, University of British Columbia, Vancouver, BC, 2025.

[3] P. C. Krause, O. Wasynczuk, and S. D. Sudhoff, *Analysis of Electric Machinery and Drive Systems*, 2nd ed., Piscataway, NJ: IEEE Press, 2002.

[4] P. Pillay and R. Krishnan, "Modeling, simulation, and analysis of permanent-magnet motor drives, part II: The brushless DC motor drive," *IEEE Trans. Ind. Appl.*, vol. 25, no. 2, pp. 274–279, Mar./Apr. 1989.

[5] P. C. Krause, O. Wasynczuk, S. Pekarek, and T. O'Connell, *Electromechanical Motion Devices: Rotating Magnetic field-based Analysis with Online Animations*. Hoboken, NJ: Wiley-IEEE Press, 2020.

[6] D.-K. Kim, K.-W. Lee, and B.-I. Kwon, "Commutation torque ripple reduction in a position sensorless brushless DC motor drive," *IEEE Trans. Power Electron.*, vol. 21, no. 6, pp. 1762–1768, Nov. 2006.

[7] Y. Liu, Z. Q. Zhu, and D. Howe, "Commutation-torque-ripple minimization in direct-torque-controlled PM brushless DC drives," *IEEE Trans. Ind. Appl.*, vol. 43, no. 4, pp. 1012–1021, Jul./Aug. 2007.

[8] R. C. Osgood, "Hall Effect Sensor Misalignment Correction in BLDC Motors," *IEEE Trans. Ind. Electron.*, vol. 58, no. 9, 2011.

[9] J. Fang, "Torque ripple minimization in BLDC motors with vector control," *IEEE Trans. Magn.*, vol. 45, no. 1, 2009.

[10] S. Song, "Averaging filter for Hall sensor error correction," *IEEE Trans. Power Electron.*, vol. 28, 2013.

[11] H. Wang, "Digital filter design for BLDC drives," *Conf. Rec. IEEE IAS*, 2015.

[12] K. I. Hwu, "Phase Advance Control for BLDC," *IEEE Trans. Power Electron.*, 2010.

[13] C. Xia, "Automatic Phase Advance," *IEEE Trans. Energy Convers.*, 2016.